Mapping the Inner Zodiacal Light with Clementine

Joseph M. Hahn
Lunar and Planetary Institute

Herbert A. Zook
Johnson Space Center

Bonnie Cooper
Oceaneering Space Systems

Bhaskar Sunkara
Lunar and Planetary Institute

March 11, 2001

Introduction

The zodiacal light is the sunlight that is reflected by interplanetary dust. This diffuse band of light is of considerable scientific interest, not just because its large extent actually makes it the most luminous component of our planetary system, but also because its light distribution upon the sky is indicative of the spatial distribution of dust throughout the solar system. In order to asses this dust distribution, numerous observations have measured the brightness of the zodiacal light on various parts of the sky. Most notable are the infrared observations by the IRAS and COBE spacecraft which have produced fairly complete maps of the outer zodiacal light (e.g, radiation from dust exterior to Earth's orbit about the Sun). However maps of the inner zodiacal light are generally less comprehensive. This is partly due to the difficulty of observing towards the Sun from the ground, since sunlight scattered by the atmosphere tends to mask the faint zodiacal light and contaminate the result, even when observing from aircraft or during eclipse.

However this situation improved considerably when the Clementine spacecraft used its star tracker camera to image the zodiacal light. Clementine orbited the Moon for about two months in early 1994, ostensibly to study the lunar surface. But a secondary objective of this mission was to image the zodiacal light using Clementine's wide-angle navigation camera. Using the Moon to eclipse the Sun, the star tracker camera repeatedly imaged the zodiacal light from the vicinity of Venus'

orbit down to about 7 solar radii; inside of this distance the zodiacal light saturated the camera's CCD detector. Hundreds of such images were acquired over a broad visual band spanning wavelengths of 0.4 to 1.1 μm during Clementine's 71 days in orbit about the Moon, and a sample image is shown in Figure 1.

Although the Moon subtends a wide swath of the zodiacal light in each image, typically $\sim 20^\circ$, it blocked different parts of the zodiacal light in images acquired at different times due to the relative motions of the spacecraft, the Moon, and the Sun. Consequently, we can combine the individual images to form a considerably larger Sun-centered map of the zodiacal light, shown in Figure 2.

The Density of Interplanetary Dust

The surface brightness of the zodiacal light constrains both the albedo p and the cross–sectional density σ of interplanetary dust. If it is assumed that the dust cross–sectional density has azimuthal symmetry and also varies radially as a power law, then we can write

$$\sigma(r,z) = \sigma_1 \left(\frac{r}{r_1}\right)^{-\nu} h(z/r) \tag{1}$$

where r is the heliocentric distance, $r_1 = 1$ AU is a reference distance, $\sigma_1 = \sigma(r_1, 0)$ is the dust cross–sectional density in the ecliptic at $r_1 = 1$ AU, and $h(z/r)$ describes how the dust–density falls off with distance z from the dust midplane. The surface brightness Z of the sunlight reflected by this dust is thus the dust surface area $\times$ its reflected light–scattering function integrated along the line–of–sight:

$$Z(\varepsilon,\theta) = \frac{\sigma_1 r_1}{\sin^{\nu+1}(\varepsilon)} \frac{p}{\pi} B_\odot \Omega_\odot \int_\varepsilon^\pi \psi(\pi - \xi) h(z/r) \sin^\nu(\xi) d\xi \tag{2}$$

where (ε, θ) are the (elongation, latitude) of the line–of–sight, $B_\odot$ is the mean surface brightness of the Sun, $\Omega_\odot$ is the solid angle of the solar disk, ψ is the dust phase law, ξ is the scattering angle, and z/r is a function of ε, θ, and ξ.

We shall adopt the empirical phase law

$$\psi(\pi - \xi) = e^{-K(\pi-\xi)} \text{ steradians}^{-1} \tag{3}$$

with $K = 0.77$, which has been shown fit other zodiacal light observations acquired over a wide range of elongation angles (Zook and Kessler 1968).

Radial Variations

If we consider a line–of–sight in the ecliptic, $h(z/r = 0) = 1$ and the integral in Eq. (2) evaluates to $\simeq 0.57$ steradians^{-1} for the range of elongations $\varepsilon < 30°$ considered here. The zodiacal light surface brightness $Z(\varepsilon, 0)$ then has a simple power–law dependence upon $\sin(\varepsilon)$:

$$Z(\varepsilon, 0) \simeq 1.2 \times 10^{-5} \frac{p\sigma_1 r_1 B_\odot}{\sin^{\nu+1}(\varepsilon)}. \tag{4}$$

The observed ecliptic surface brightness $Z(\varepsilon, 0)$ is plotted in Figure 3., which demonstrates that the zodiacal light's midplane does indeed vary as a single power law $Z(\varepsilon, 0) = 2.3 \times 10^{-13} B_\odot / \sin^{\nu+1}(\varepsilon)$ with $\nu = 1.43 \pm 0.05$. Comparison with Eq. (4) thus provides a constraint on the dust–density×albedo: $p\sigma_1 r_1 = 1.9 \times 10^{-8}$.

Vertical Variations

To extract the dust vertical distribution, we must choose a functional form for $h(z)$ and integrate Eq. (2) numerically. We adopt the function

$$h(z/r) = e^{-k_1|\sin(z/r)|^{k_2}}, \tag{5}$$

a form that is quite common in the zodiacal light literature (Zook and Kessler 1968, Leinart 1975).

Figure 4. shows a fit of the model to the observed zodiacal light isophotes. The model's vertical parameters are $k_1 = 1.15 \pm 0.1$ and $k_2 = 1.40 \pm 0.1$. It should be noted that we have not yet explored alternate forms for the dust vertical distribution, Eq. (5), so the uniqueness of this fit is uncertain. From this fit, we shall derive the inclination distribution (or distributions) for the interplanetary dust complex, which will hopefully provide an indicator of the relative importance of the various sources of this dust (e.g., low–inclination asteroids and/or high–inclination comets?).

Preliminary Findings

- Using the Moon to occult the Sun, the Clementine spacecraft used its wide–angle navigation cameras to image the inner zodiacal light over elongations of $2^\circ \lesssim \varepsilon \lesssim 30^\circ$. This yielded the first comprehensive map of the inner zodiacal light (shown in Figure 2.) obtained using a modern CCD–based camera.

- A comparison of the observed ecliptic surface brightness (Figure 3.) to theory [Eq. (4)] shows that the interplanetary dust density falls off with heliocentric distance r as $r^{-1.43\pm0.05}$.

- The isophotes of the zodiacal light are consistent with the vertical distribution given in Eq. (5) with the parameters $k_1 = 1.15 \pm 0.1$ and $k_2 = 1.40 \pm 0.1$. This distribution will be inverted to extract the inclination distribution of these dust grains. However the uniqueness of this solution is still unknown.

- The dust albedo $p \times$ the dust cross–sectional density σ_1 at $r_1 = 1$ AU obeys $p\sigma_1 \simeq 1.3 \times 10^{-21}$ cm^{-1}.

  - If we assume a characteristic asteroidal albedo of $p \simeq 0.08$, the dust cross–sectional density is $\sigma_1 \simeq 1.6 \times 10^{-20}$ cm^2/cm^3, which also agrees with measurements of dust impacts upon spacecraft (Zook *et al.* 1970).

  - Most of this cross–section is contributed by grains having radii $R \sim 30$ μm (Zook *et al.* 1970), so the number–density of these grains is $n \sim \sigma_1/\pi R^2 \sim 6 \times 10^{-16}$ cm^{-3} which have a mass–density of $\sim 4\pi\rho R^3 n/3 \sim 1 \times 10^{-22}$ gm/cm^3 assuming a dust bulk–density of $\rho \sim 2$ gm/cm^3. It should be noted that this mass–density estimate is a lower limit since these observations are rather insensitive to rare grains that may be considerably larger than $R \sim 30$ μm that may contribute very little optical depth yet may still carry considerable mass.

Preprint Requests

References

Leinart, C. 1975, Zodiacal light—a measure of the interplanetary environment. *Space Science Reviews*, **18**, 281.

Zook, H. A. and D. J. Kessler, 1968, Interplanetary dust: the zodiacal light and meteoroid measurements. *OART–OSSA Meteoroid Environment Workshop*, 355.

Zook, H. A., R. E. Flaherty, and D. J. Kessler, 1970, Meteoroid impact on the Gemini windows, *Planet. Space Sci.*, **18**, 953.

Figure 1. A sample image of the zodiacal light observed by the Clementine startracker camera. The field is $45^\circ \times 30^\circ$ wide with ecliptic north and east being up and left. The Sun is two degrees behind the lunar horizon, and a saturated Venus is the bright object left of the Moon. The greyscale shows the zodiacal light via a logarithmic stretch and the Moon via a linear stretch.

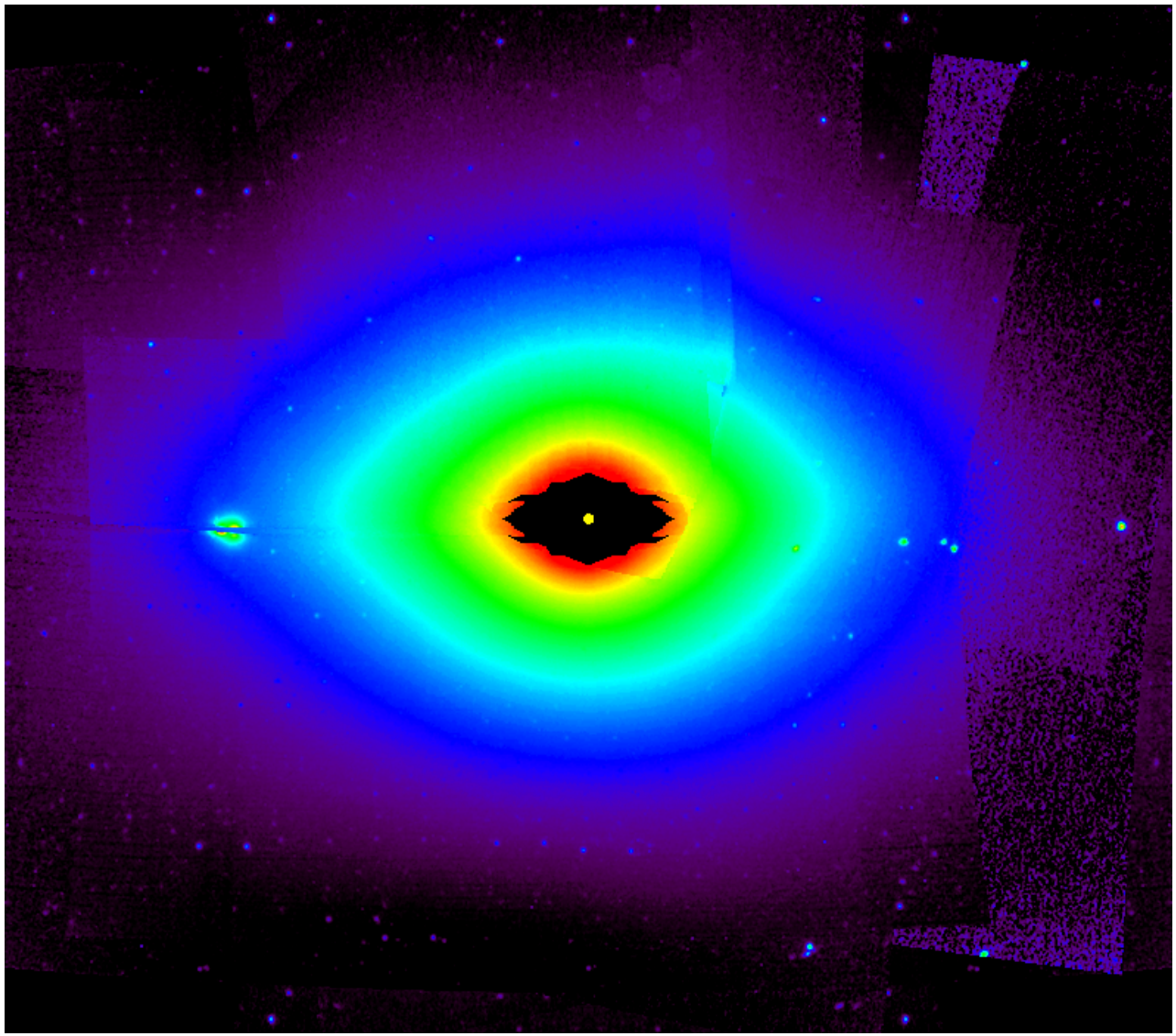

Figure 2. A mosaic of six fields–of–view of the zodiacal light. This mercator projection is $60^\circ \times 50^\circ$ with ecliptic east to the left and ecliptic north up. The far west fields are the noisiest due to their short integration times. These images were acquire over a five week interval, so the stars drift to the right with time and some planets appear at multiple longitudes. A saturated Venus lies about 20° east (left) of the Sun, and Saturn is barely discernible at about 12° west. Mars appears at 17° and 19° west, Saturn again at 20°, and Mercury at 28° west.

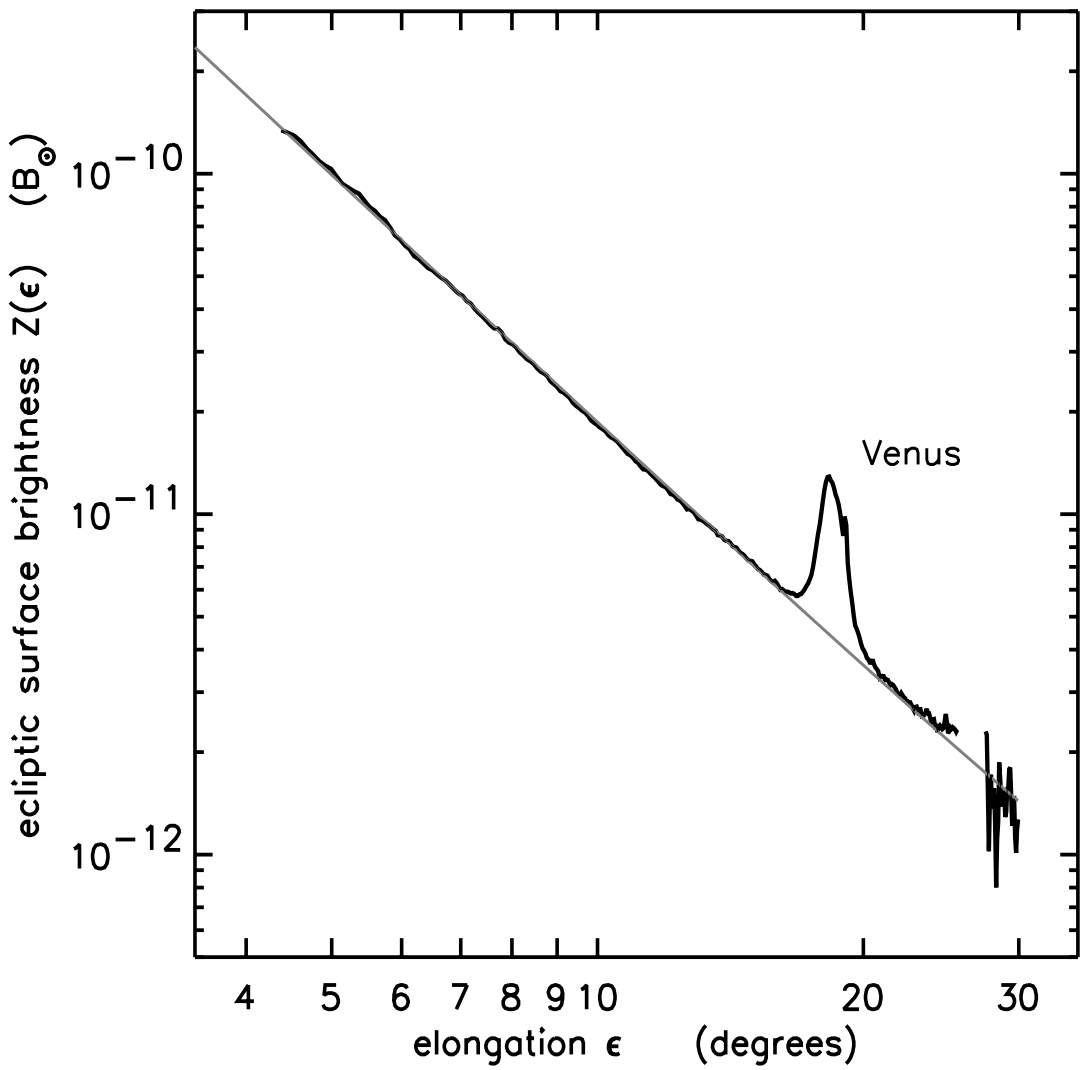

Figure 3. The surface brightness of the zodiacal light $Z(\varepsilon)$ versus elongation angle ε along the ecliptic and east of the Sun, in units are the mean solar brightness $B_\odot$. The grey curve is the power–law fit $Z(\varepsilon) = 2.3 \times 10^{-13} B_\odot / \sin^{(\nu+1)}(\varepsilon)$ with $\nu + 1 = 2.43 \pm 0.05$.

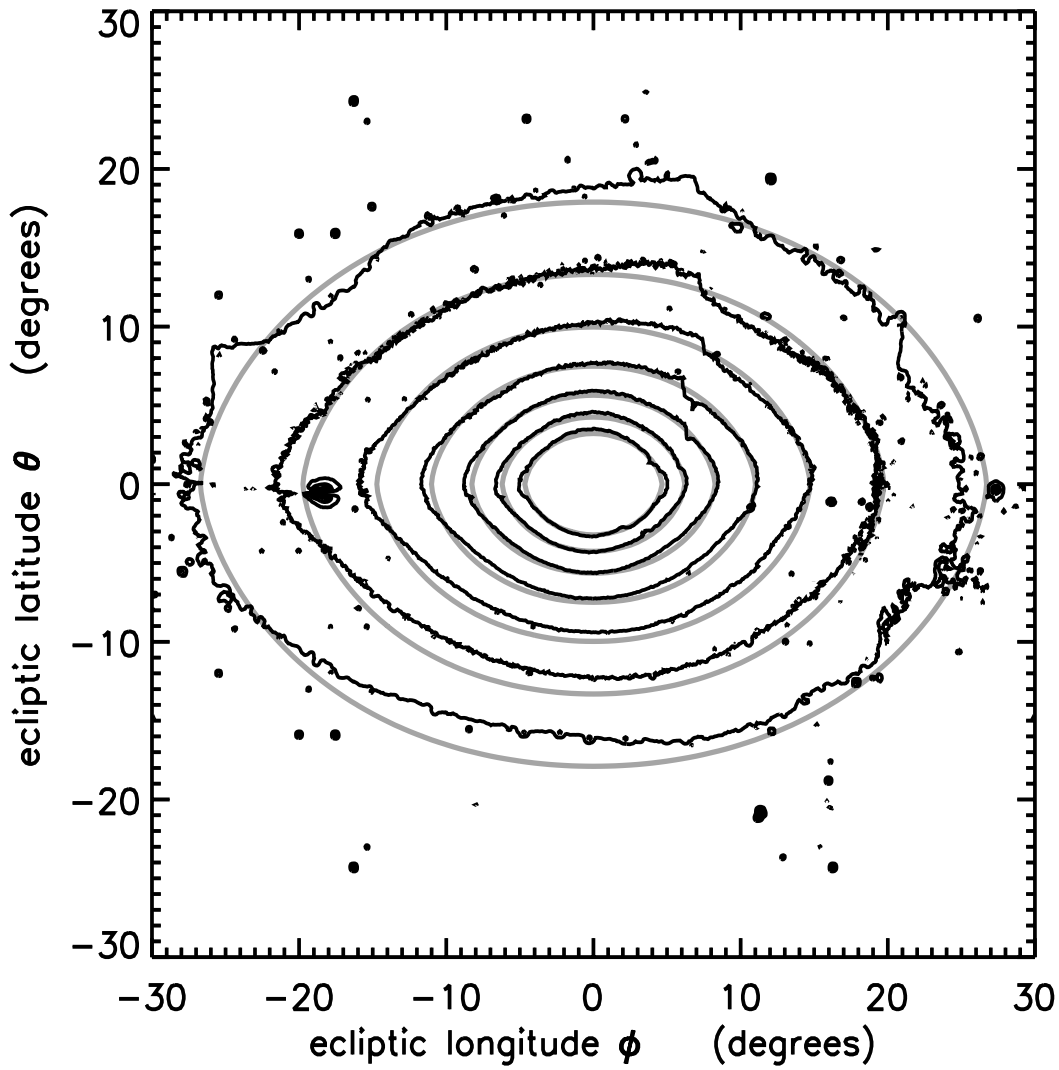

Figure 4. The dark curves are isophotes for the zodiacal light map seen in Figure 1. Adjacent contours differ in brightness by a factor of 2. The grey curves are the model having parameters $p\sigma_1 r_1 = 1.9 \times 10^{-8}$ and a dust radial power–law $\nu = 1.43$ and $k_1 = 1.15$, and $k_2 = 1.40$ for the dust vertical distribution.